Catalysis Letters Vol. 105, Nos. 3–4, December 2005 (© 2005)
DOI: 10.1007/s10562-005-8697-2

A comparison of oxygen-vacancy effect on activity behaviors of carbon dioxide and steam reforming of methane over supported nickel catalysts

Ta-Jen Huang*, Han-Jun Lin, and Tien-Chun Yu

Department of Chemical Engineering, National Tsing Hua University, Hsinchu, Taiwan 300, ROC

Received 27 June 2005; accepted 12 September 2005

A comparison of the activity behaviors of the mechanistically similar reactions of carbon dioxide reforming and steam reforming of methane was carried out at 400∼550 °C over nickel catalysts with samaria- and gadolinia-doped ceria and α-alumina as the supports. Results show that the activity behaviors of carbon dioxide reforming and steam reforming of methane are similar and very sensitive to the oxygen-vacancy properties of the support, with a drastic increase of the activities as the temperature increases from 450 to 500 °C. Nevertheless, a difference in the activity behaviors between carbon dioxide and steam reforming has been observed and is due to a difference in the reaction mechanisms of CO_2 and H_2O dissociations. Possible carbon deposition (coking) is lessened due to the reaction of the surface carbon species with the lattice oxygen or the surface O species as produced from CO_2 or H_2O. It was found that the samaria-doped ceria supported nickel catalyst has better de-coking ability than that of the gadolinia-doped ceria supported one. An oxygen-transport reaction mechanism for doped-ceria supported Ni catalyst has been proposed and shown to explain the activity behaviors successfully.

KEY WORDS: oxygen vacancy; carbon dioxide reforming; steam reforming; activity behavior; methane; doped ceria; nickel catalyst.

1. Introduction

Steam reforming of methane has been employed for large scale production of hydrogen. Nickel catalyst has been found to exhibit promising catalytic performance for steam reforming of methane [1,2]. On the other hand, the reforming of methane with carbon dioxide to synthesis gas has gained growing interest partially due to environmental implications, since both methane and carbon dioxide are greenhouse gases, and partially due to the produced synthesis gas having a low H_2:CO ratio, which is of particular interest to the synthesis of valuable oxygenated chemicals. Nickel catalyst has also been found to exhibit promising catalytic performance for carbon dioxide reforming of methane [3–5]. It is interesting to note that these reacions of steam reforming and carbon dioxide reforming of methane have been found to be mechanistically similar [6]. Thus, their activity behaviors are conceivably to be similar.

The effect of the support on steam reforming of methane over nickel catalysts has been studied [2,7]. Strong metal–support interaction (SMSI) has been shown to play a very important role in the catalytic activity of these nickel catalysts. On the other hand, the effect of the support on carbon dioxide reforming of methane over nickel catalysts has also been studied [8–10]. These studied supports were all oxygen-ion conducting materials, which own oxygen vacancies. Thus, the SMSI is presumably due to the interaction of the surface oxygen vacancies of the support with the supported nickel metal. In this work, the doped ceria is employed as the oxygen-ion conducting material and its oxygen-vacancy properties are varied with different dopants, i.e. samaria and gadolinia. Since α-alumina (α-Al_2O_3) has no oxygen vacancy, it was employed in this work to help the verification of the oxygen-vacancy effect of the doped ceria.

In this work, the effects of the oxygen-vacancy properties of the support on activity behaviors of carbon dioxide and steam reforming of methane over the doped-ceria supported nickel catalysts have been studied. Results show a difference in the activity behaviors of the mechanistically similar reactions of carbon dioxide reforming and steam reforming. An oxygen-transport reaction mechanism for doped-ceria supported Ni catalyst has been proposed and shown to explain the activity behaviors successfully.

2. Experimental

2.1. Preparation of doped ceria

Samaria-doped ceria (SDC) was prepared by a co-precipitation method from reagent-grade (99.999% purity, Strem Chemical) metal nitrates $Sm(NO_3)_3{\cdot}6H_2O$ and $Ce(NO_3)_3{\cdot}6H_2O$. Appropriate amounts of samarium nitrate and cerium nitrate, corresponding to an atomic molar ratio of Sm:Ce = 1:9, were dissolved in de-ionized water to make 0.08 M solutions. Hydrolysis of

* To whom correspondence should be addressed.
E-mail: tjhuang@che.nthu.edu.tw

the metal salts to hydroxides was obtained by slowly dropping each such solution into NH_4OH solution and in the meantime stirring to keep the pH of the solution >9. A distinct deep purple color of precipitate/gel was formed when the nitrate solution was dropped into NH_4OH. Vacuum filtration was employed to isolate the gel, which was then washed twice by water and ethanol. After washing, the gel was dried under vacuum at 110 °C for 4 h, calcined in air at 300 °C for 2 h and then at 600 °C for 4 h, and then slowly cooled down to room temperature.

Gadolinia-doped ceria (GDC) was prepared with the same method. The atomic molar ratios of Gd:Ce for GDC was also 1:9.

2.2. Preparation of doped-ceria supported nickel catalyst

The doped-ceria supported nickel catalyst was prepared by impregnating the above-prepared doped ceria with an appropriate amount of aqueous solution of nickel nitrate trihydrate, $Ni(NO_3)_2{\cdot}3H_2O$ (99.999% purity, SHOWA, Japan) for 7 h. After evaporating excess water at 80 °C, the catalysts were dried under vacuum at 80 °C for 12 h, and then calcined in air at 260 °C for 1.5 h and then at 500 °C for 3.5 h. The calcination of the supported nickel catalyst was conducted by passing air at a rate of one l/min, and by ramping the temperature at a rate of 10 °C/min.

In this work, the nickel catalyst is always supported and with a loading of 2 wt% with respect to the weight of the support.

2.3. Temperature-programmed reduction

Temperature-programmed reduction (TPR) was carried out by using 10% hydrogen in argon as a reducing gas in a conventional TPR reactor. The reactor was made up of an 8-mm-I.D. quartz U-tube with sample of 100 mg mounted on loosely packed quartz wool. The outlet of the reactor was connected to a glass column packed with molecular sieve 5A in order to remove the moisture produced by reduction. The flow rate of the reducing gas was kept at 30 ml/min by a mass flow controller. The temperature of the reactor was ramped from room temperature to 900 °C at a rate of 10 °C / min by a temperature programmable controller (Eurotherm, Model 815P). The rate of hydrogen consumption was measured by a thermal conductivity detector and recorded by an on-line personal computer. The peak areas of TPR were separated and integrated using software developed by SISC, Taiwan.

2.4. Activity tests of carbon dioxide and steam reforming of methane

The activity tests for carbon dioxide reforming and steam reforming of methane were conducted at 350∼550 °C (623∼823 K) under atmospheric pressure in the same reactor as that of the foregoing dissociation tests. The Ni/GDC and Ni/SDC catalysts with 2 wt% Ni were used. The Ni/α–alumina catalyst with 2 wt% Ni was also used for comparison. The gas feed was passed through an oxygen filter to eliminate trace amounts of oxygen. The test started with H_2 pre-reduction of the catalyst. A mixture of CH_4:CO_2:Ar = 25:25:50 for carbon dioxide reforming, or CH_4:H_2O:Ar = 25:25:50 for steam reforming, was then fed to the catalyst bed at a total flow rate of 100 ml/min. The reactor outflow of each reaction was analyzed on-line by gas chromatograph (China Chromatograph 8900, Taiwan) and CO-NDIR (Beckman 880). The rate of carbon formation was measured by temperature-programmed oxidation after each activity test, as detailed in the following section.

2.5. Temperature-programmed oxidation

Temperature-programmed oxidation (TPO) of the reforming tested catalyst was carried out by using 20% oxygen in argon as an oxidizing gas in a reactor which was made up of an 8-mm-I.D. quartz U-tube with sample of 100 mg mounted on loosely packed quartz wool. The flow rate of the oxidizing gas was kept at 100 ml/min by a mass flow controller. The temperature of the reactor was ramped from room temperature to 900 °C at a rate of 10 °C/min by a temperature programmable controller (Eurotherm, Model 815P). The amount of carbon dioxide production was measured by a CO_2-NDIR and recorded by an on-line personal computer. The peak area of TPO was integrated using software developed by SISC, Taiwan.

3. Results and discussion

3.1. Oxygen-transport reaction mechanism with Ni/doped ceria

A schematic diagram of production, transport, and reaction of the mobile oxygen species for carbon dioxide (CO_2) reforming of methane (CH_4) over doped-ceria supported Ni catalyst is proposed as shown in figure 1. This is called "oxygen-transport reaction mechanism" in this work. Note that the left-hand side of this diagram, on the reaction scheme of CO_2 reforming of CH_4 over Ni and Ni-vacancy interface, has been reported by our laboratory [8] and the rest of it, i.e. CO_2 dissociates over the oxygen vacancy to produce CO and the produced O species is transported into the bulk and to the oxygen vacancy–Ni interface, is similar to that for steam reforming of methane over ceria [11] and will be verified in the following.

It is seen in figure 1 that CO_2 dissociation produces gaseous CO and atomic oxygen, which occupies an oxygen vacancy. Note that the dissociation of CO_2 over

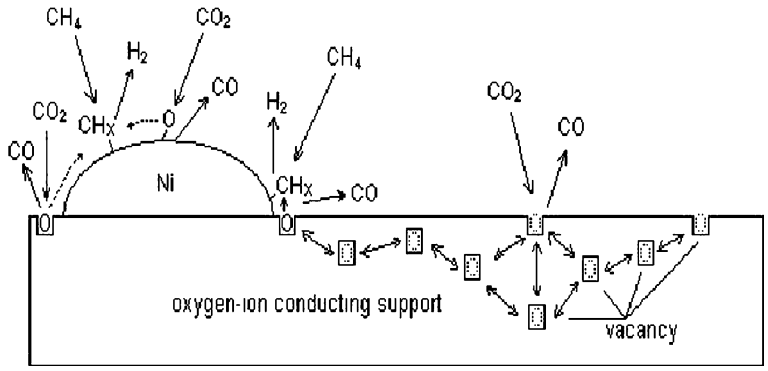

Figure 1. A schematic diagram of production, transport, and reaction of the mobile oxygen species for CO_2 reforming of CH_4 over doped-ceria supported Ni catalyst.

doped ceria has been considered as $CO_2 \rightarrow CO + O$ [12], which is the same as that over the reduced ceria [13]. The produced O species has been considered to occupy the oxygen vacancy at one to one ratio, i.e. an atomic oxygen species occupies an oxygen vacancy [12].

According to the oxygen-transport reaction mechanism of figure 1 and for kinetic consideration, the oxygen-vacancy properties considered in this work are the oxygen-ion conductivity and the density of the surface oxygen vacancies, with the latter corresponding to the density of the interfacial Ni–vacancy sites. As reported by Huang and Yu [12] for CO_2 reaction over Ni/GDC and Ni/SDC, as the reaction temperature increases from 450 to 500 °C, the oxygen-ion conductivity becomes high enough so that the lattice oxygen becomes mobile and thus the bulk oxygen vacancies become available to take in the produced O species from the CO_2 dissociation; as a consequence, the CO_2 dissociation activity has a drastic increase. Since the produced O species occupy the oxygen vacancy at one to one ratio, this drastic increase of the CO_2 dissociation activity is an indication of a drastic increase of the available amount of the oxygen vacancies for the reaction. In addition, it has been reported [12] that the oxygen-ion conductivity of SDC is higher than that of GDC but the density of the surface oxygen vacancies of SDC is lower than that of GDC.

Note that for Ni/α–alumina, the oxygen-transport reaction mechanism of figure 1 also works but without the oxygen vacancies, i.e. both CH_4 and CO_2 dissociations occur over Ni and the produced O species from CO_2 dissociation may transport over the Ni surface to react with the CH_x species.

3.2. *Activity behavior of carbon dioxide reforming of methane*

Figure 2 shows that both CH_4 conversion and CO_2 conversion in CO_2 reforming of methane are very sensitive to the oxygen-vacancy properties of the support. Note that α-Al_2O_3 has no oxygen vacancy. As temperature increases from 450 to 500 °C (723 to 773 K), a sharp increase of the difference between the activities of the doped-ceria supported Ni catalyst and that of α-Al_2O_3 supported one occurs and is considered to be due to the above-described drastic increase of the available amount of the oxygen vacancies. This increase in difference between activities is also true for hydrogen (H_2) production, as shown in figure 3. Note that the profile of H_2 production rate is able to reflect the activity behavior of the CO_2 reforming of methane if the reaction is considered as $CH_4 + CO_2 \rightarrow 2\,H_2 + 2\,CO$.

The above-described increase in difference between activities is considered to be due to that the effect of the oxygen vacancies is to increase not only the CO_2 dissociation activity as described above but also the conversion of the adsorbed carbon species, i.e., CH_x, via the oxygen-transport reaction mechanism of figure 1. This greatly increases the CH_4 conversion, which produces hydrogen, and also lessens the carbon deposition, as will be discussed later. The CO_2 conversion rate is thus further enhanced due to the consumption of the produced oxygen species. As a consequence, CH_4 conversion, CO_2 conversion, and H_2 production rate of the doped-ceria supported Ni catalysts all increase drastically as compared to those of the α-Al_2O_3 supported one.

Figures 2 and 3 also show that, above 723 K (450 °C), the difference broadening between the activities of the doped-ceria supported Ni catalyst and that of α–Al_2O_3 supported one increases with an increase of the reaction temperature. This indicates the effect of the oxygen-ion conductivity of the support on the reaction over the Ni catalyst. As schematically shown in figure 1, higher mobility of the lattice oxygen will lead to higher activity of the methane reaction. Note that as the reaction temperature increases, the oxygen-ion conductivity increases, i.e. the mobility of the lattice oxygen increases.

It is also shown in Figures 2 and 3 that, as the temperature increases to 550 °C (823 K), the activities of CH_4 conversion, CO_2 conversion, and H_2 production over GDC supported Ni catalyst are all higher than those over SDC supported one, while they are all

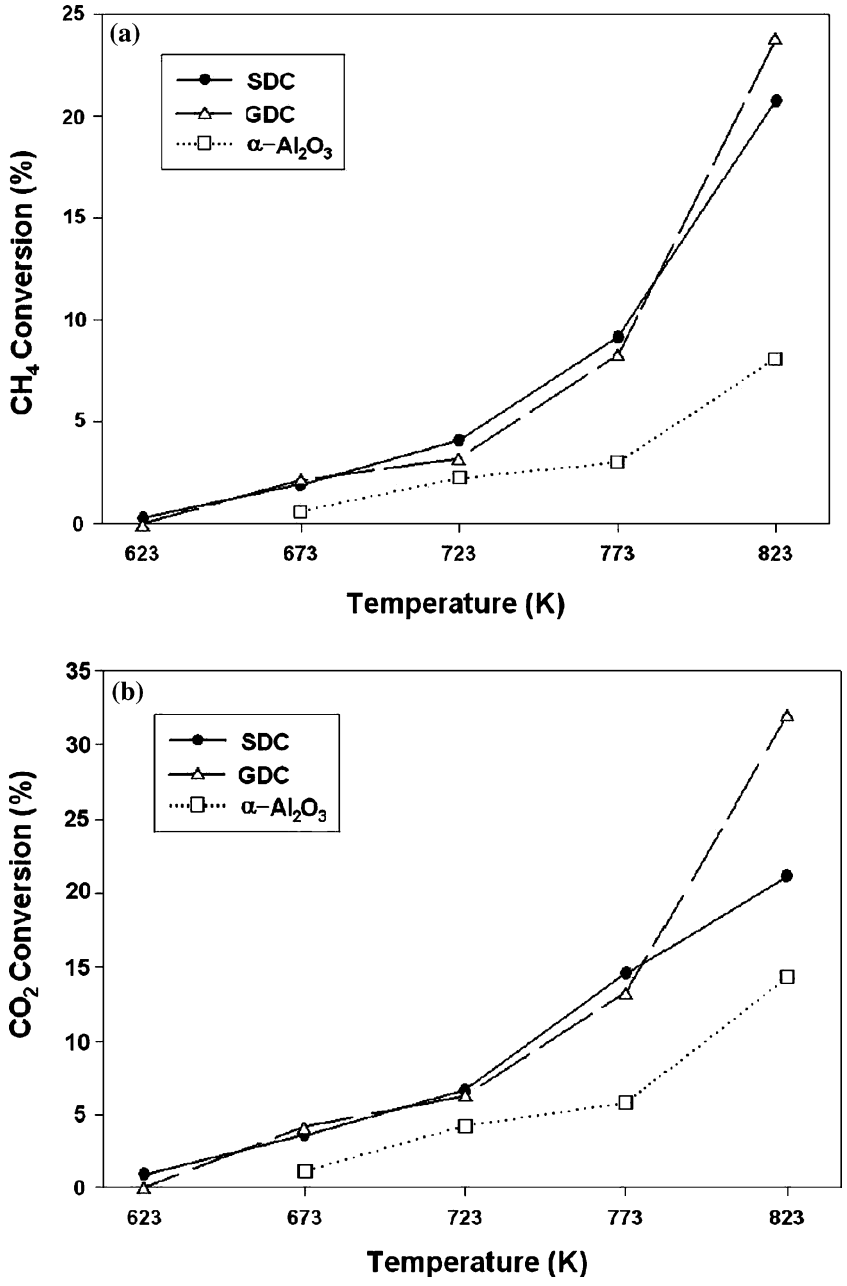

Figure 2. Activity profiles for CO_2 reforming of methane over Ni catalyst supported on various materials as indicated. (a) CH_4 conversion, (b) CO_2 conversion.

slightly lower at temperatures of 500 °C (773 K) or lower. This is considered to be due to that the density of the interfacial active centers over GDC is higher than that over SDC. Noting that the interfacial active center is formed at the interface of Ni and oxygen vacancy, the higher density of the surface oxygen vacancies of GDC leads to a higher density of its interfacial active centers than that of SDC. For temperatures lower than 500 °C, the slightly lower activities are considered to be due to the lower oxygen-ion conductivity of GDC than that of SDC. The reason why the oxygen-ion conductivity of GDC does not limit its activities at 550 °C is considered to be that the increase of the temperature increases the oxygen-ion conductivity and there is high enough oxygen-ion conductivity at 550 °C to carry out the oxygen-transport reaction mechanism of figure 1 so that the transport of the oxygen species will not be the rate-determining step in the reaction sequence.

On the other hand, at temperatures of 450 °C (723 K) or lower, it is also seen in figures 2 and 3 that the activities of CH_4 conversion, CO_2 conversion, and H_2 production over the doped-ceria supported Ni catalyst all have similar behaviors as those over α–Al_2O_3 supported one. Note that α-Al_2O_3 has lower BET surface

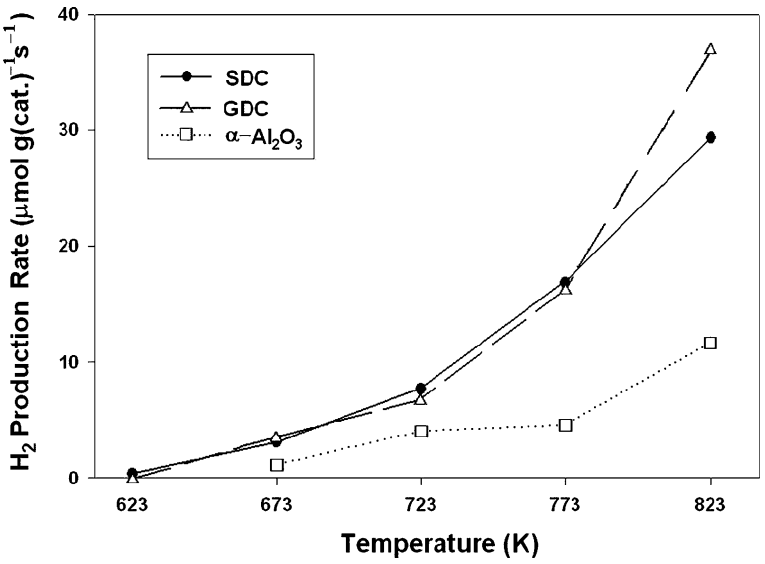

Figure 3. Hydrogen production profile for CO_2 reforming of methane over Ni catalyst supported on various materials as indicated.

area, which is 6 m^2/g, than those of GDC and SDC, which are about the same at 40 m^2/g, and thus its Ni dispersion may be lower which may lead to lower activity. This shows that, at these low temperatures, the oxygen vacancies may have only small effect on the activities. There is no synergistic effect from CO_2 dissociation at the surface oxygen vacancies other than those at the Ni–vacancy interface. This is an indication that the oxygen transport mechanism of figure 1 is important on the activity increase, as discussed above. At low temperatures, the oxygen-ion conductivity is low and thus the mobility of the lattice oxygen may be low enough for the oxygen transport mechanism to take no effect.

3.3. *A comparison of activity behaviors of carbon dioxide and steam reforming*

Figures 4 and 5 show that, for steam reforming of methane, CH_4 conversion, H_2O conversion, and H_2 production rate are all very sensitive to the oxygen-vacancy properties of the support, especially at temperatures higher than 723 K (450 °C) when the effect of the oxygen vacancies increases drastically. The CH_4 and H_2O conversions over GDC are higher than those over SDC, especially at temperatures higher than 773 K (500 °C), showing the same trend as for carbon dioxide reforming of methane. However, at temperatures higher than 773 K, it is also seen that the activities of CH_4 conversion and H_2 production for steam reforming are not going up as much as those for CO_2 reforming but rather going flattened. This is considered to be due to different reaction mechanisms of H_2O and CO_2 dissociation over the doped-ceria supported nickel catalyst, as discussed in the following.

For CO_2 dissociation over the doped ceria, the reaction is considered to be the same as that over the reduced ceria [13], which is the same as that over the nickel metal [14], i.e.

$$CO_2 + {}^* \rightarrow CO + O^* \quad (1)$$

where * denotes an active site over nickel or an oxygen vacancy over ceria or is considered as an active site over the reduced ceria, and O^* denotes an adsorbed oxygen species over nickel or an occupied oxygen vacancy or is considered as an oxidized ceria species [13]. Note that reaction (1) is the same as what we have proposed in section 3.1 and consistent with the mechanism of "CO_2 dissociates over the oxygen vacancy to produce CO and the O species" as shown in figure 1. Thus, for CO_2 dissociation over the doped ceria, the produced oxygen species may be immediately transported to the interfacial active center via the oxygen-ion conducting support or diffuse over the nickel surface to oxidize the adsorbed carbon species, as schematically shown in figure 1. Note that the oxygen-ion conductivity increases drastically with increasing temperature over 723 K (450 °). This leads to the drastically increased activities with temperature as shown in Figures 2 and 3.

On the other hand, the reaction for H_2O dissociation over the doped ceria is also considered to be the same as that over the reduced ceria [11], i.e.

$$H_2O + {}^* \rightarrow H_2 + O^* \quad (2)$$

This is the same as that for H_2O dissociation over the nickel metal [15]. Nevertheless, it is reported that the produced oxygen species promotes the autocatalytic H_2O dissociation [15], i.e.

$$H_2O + {}^* + O^* \rightarrow H_2 + 2O^* \quad (3)$$

However, as the Ni sites become occupied by the O species as the temperature increases, i.e. as the concentration of O^* increases to some extent, the reaction slows down [15]. This is exactly the activity behavior as shown

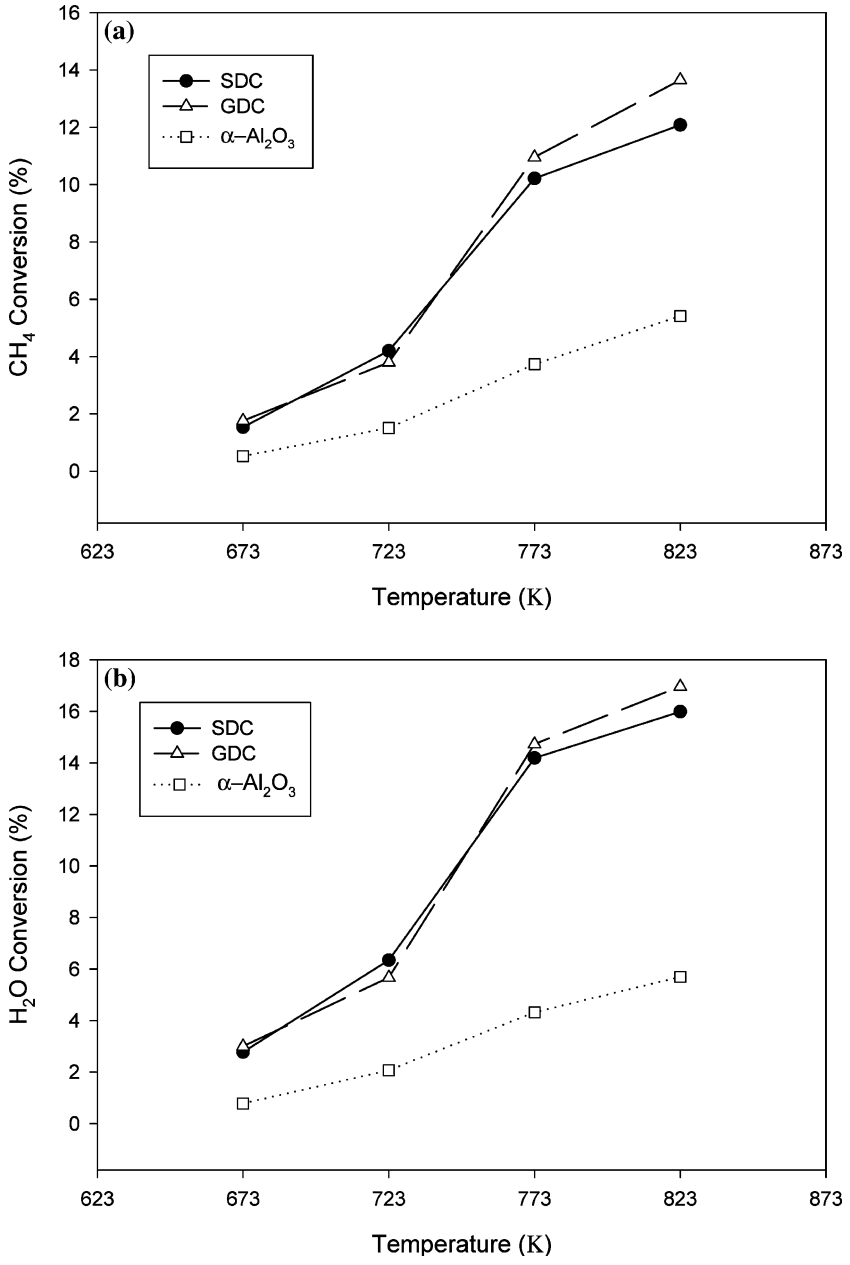

Figure 4. Activity profiles for steam reforming of methane over Ni catalyst supported on various materials as indicated. (a) CH_4 conversion, (b) H_2O conversion.

in figure 4(b), where the H_2O conversion slows down at temperature over 773 K. This in turn causes CH_4 conversion and H_2 production for steam reforming to slow down, i.e. their activities to go flattened as shown in Figures 4(a) and 5. Note that steam reforming of methane is considered to occur as $CH_4 + H_2O \rightarrow CO + 3\ H_2$.

The above-observed difference in the activity behaviors of H_2O and CO_2 dissociation may be due to a small difference in their reaction mechanisms. For H_2O dissociation over ceria, the reaction is [16]

$$H_2O + {}^* + O^* \rightarrow 2HO^* \quad (4)$$

At temperature above 500 K, the following reaction occurs [17]:

$$2HO^* \rightarrow H_2 + 2O^* \quad (5)$$

A combination of reactions (4) and (5) yields reaction (3). Thus, for H_2O dissociation, the effect of the produced oxygen species promoting the autocatalytic H_2O dissociation over nickel may be considered to be the same as that of the occupied oxygen vacancy or the oxidized ceria site helping the adsorption of the produced hydrogen species onto ceria, i.e. $H + O^* \rightarrow HO^*$. This effect is not considered to occur for CO_2 dissociation and thus there is presumably no slowing down of

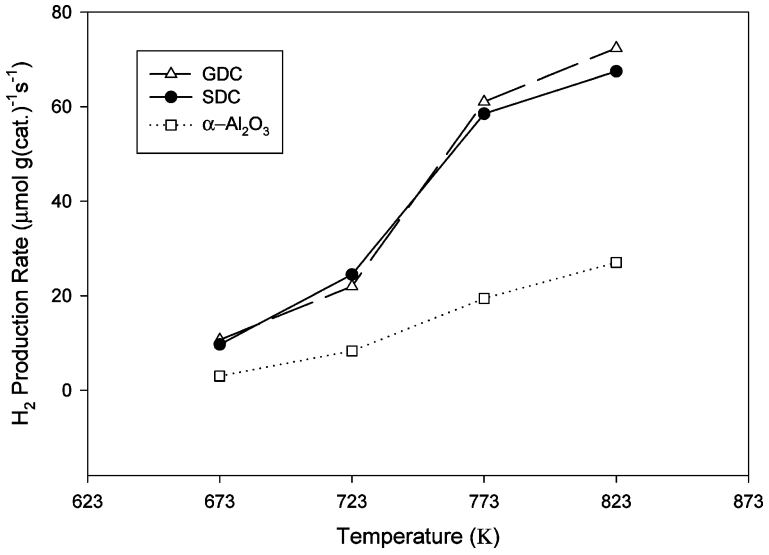

Figure 5. Hydrogen production profile for steam reforming of methane over Ni catalyst supported on various materials as indicated.

the CO_2 dissociation rate, as observed in figure 2(b). The above-mentioned small difference is thus considered to be the occurrence of the hydroxyl species in the reaction mechanism of H_2O dissociation but not in that of CO_2 dissociation. This is consistent with the finding that the formation of the surface hydroxyl species during H_2O dissociation inhibits the followed CH_4 decomposition [12].

3.4. *Effect of oxygen vacancy on de-coking activity*

Figure 6 shows that, for steam reforming of methane, the carbon formation rate is much lower over the doped-ceria supported Ni catalysts than that over α-Al_2O_3 supported one. This rate of carbon formation was measured by temperature-programmed oxidation after each activity test of carbon dioxide or steam reforming of methane; thus, a lower rate of carbon formation is corresponding to a lower of the possible carbon deposition (coking) rate. A similar behavior is observed in this work for CO_2 reforming of methane. This is due to the interfacial reaction of surface carbon species with surface O species such as

$$CH_x + O \rightarrow CO + xH \qquad (6)$$

as shown at the Ni-oxygen vacancy interface in figure 1. These surface O species may be supplemented by the lattice oxygen species as produced from CO_2 via reaction (1) or from H_2O via reaction (2). Note that α-Al_2O_3 has no oxygen vacancies and thus no function of O species supplementation from the lattice oxygen. Also note that methane is not adsorbed onto doped ceria or α-Al_2O_3 and the possible carbon deposition is due solely to CH_4 conversion over Ni.

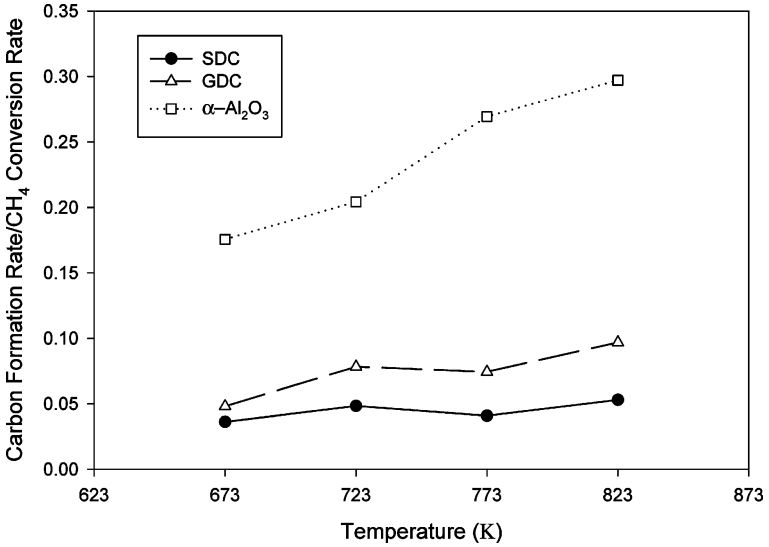

Figure 6. Carbon formation profile for steam reforming of methane over Ni catalyst supported on various materials as indicated.

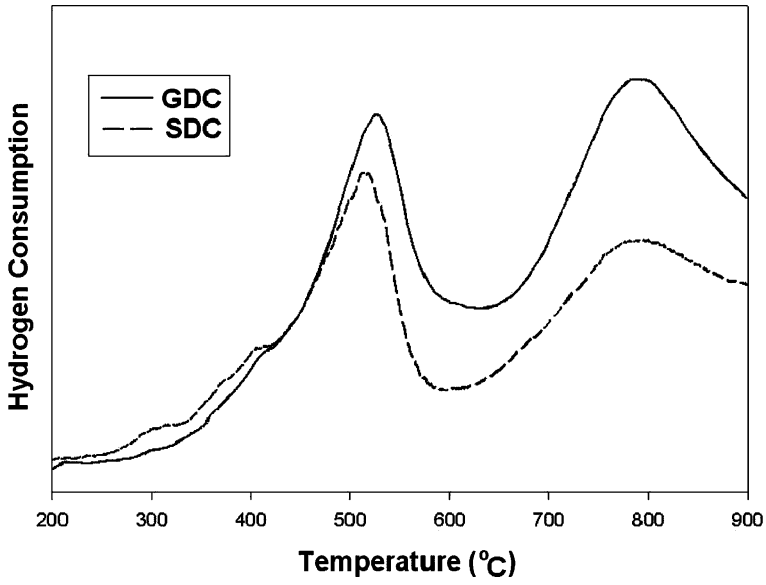

Figure 7. Temperature-programmed reduction profiles for GDC and SDC.

Figure 6 also shows that, as the temperature increases, the difference between the carbon formation rate over the doped-ceria supported Ni catalysts and that over α-Al_2O_3 supported one increases. This is considered to be due to the effect of the oxygen-ion conductivity, the same as discussed above for the activity behaviors. Thus, the existence of the Ni–oxygen vacancy interface and the O species supplementation rate are both very important for the lessening of the coking rate.

It is also seen in figure 6 that the carbon formation rate over SDC-supported Ni catalyst is lower than that over GDC-supported one. This indicates that the de-coking activity of SDC-supported catalyst is higher than that of GDC-supported one. This different decoking ability is considered to be due to a different interaction of the oxygen vacancy over different doped ceria with the surface O species which enhances the reaction of the surface O species with the surface carbon species, as discussed below. This different interaction of the oxygen vacancy with the O species may be interpreted from the TPR behaviors of GDC and SDC, as shown in figure 7, where the lower-temperature peak indicates the reduction of the surface capping oxygen and the higher-temperature peak indicates the bulk reduction. It is seen that the lower-temperature peak is at about 510 °C for SDC and at 525 °C for GDC. This difference of about 15 °C in the TPR peak temperature can mean a large difference in the reactivity and thus the interaction if the activation energy is high. In any case, a lower temperature of the reduction of the surface capping oxygen by hydrogen may lead to a lower temperature of the reduction of the surface capping oxygen by the carbon species. Thus, the SDC-supported catalyst, with a lower TPR peak temperature, may possess a higher activity for the reaction of the surface O species with the surface carbon species and result in a higher de-coking activity.

4. Conclusions

1. The activity behaviors of carbon dioxide reforming and steam reforming of methane are similar and very sensitive to the oxygen-vacancy properties of the support, with a drastic increase of the activities as the temperature increases from 450 to 500 °C.
2. A difference in the activity behaviors between carbon dioxide and steam reforming of methane has been observed and is due to a difference in the reaction mechanisms of CO_2 and H_2O dissociations.
3. Possible carbon deposition (coking) is lessened due to the reaction of surface carbon species with the lattice oxygen or the surface O species as produced from CO_2 or H_2O.
4. Samaria-doped ceria supported nickel catalyst has better de-coking ability than that of gadolinia-doped ceria supported one.
5. The proposed oxygen-transport reaction mechanism has been shown to explain the activity behavior successfully not only for CO_2 reforming of methane but also for H_2O reforming of methane over the doped-ceria supported Ni catalyst.

References

[1] H.S. Roh, K.W. Jun, W.S. Dong, J.S. Chang, S.E. Park and Y.I. Joe, J. Mol. Catal. A 181 (2002) 137.
[2] Y. Matsumura and T. Nakamori, Appl. Catal. A 258 (2004) 107.

[3] M.J. Hei, H.B. Chen, J. Yi, Y.J. Lin, Y.Z. Lin, G. Wei and D.W. Liao, Surf. Sci. 417 (1998) 82.
[4] A.A. Lemonidou and I.A. Vasalos, Appl. Catal. A 228 (2002) 227.
[5] Z. Hao, H.Y. Zhu and G.Q. Lu, Appl. Catal. A 242 (2003) 275.
[6] J.R. Rostrup-Nielsen and J.H. Bak Hansen, J. Catal. 144 (1993) 38.
[7] W.S. Dong, H.S. Roh, K.W. Jun, S.E. Park and Y.S. Oh, Appl. Catal. A 226 (2002) 63.
[8] J.B. Wang, S.Z. Hsiao and T.J. Huang, Appl. Catal. A 246 (2003) 197.
[9] J.B. Wang, L.E. Kuo and T.J. Huang, Appl. Catal. A 249 (2003) 93.
[10] J.B. Wang, Y.S. Wu and T.J. Huang, Appl. Catal. A 272 (2004) 289.
[11] E. Ramirez-Cabrera, A. Atkinson and D. Chadwick, Appl. Catal. B 47 (2004) 127.
[12] T.J. Huang and T.C. Yu, Catal. Lett., in press.
[13] S. Sharma, S. Hilaire, J.M. Vohs, R.J. Gorte and H.W. Jen, J. Catal. 190 (2000) 199.
[14] V.C.H. Kroll, H.M. Swaan, S. Lacombe and C. Mirodatos, J. Catal. 164 (1997) 387.
[15] R.V. Kasza, K. Griffiths, J.G. Shapter, P.R. Norton and D.A. Harrington, Surf. Sci. 356 (1996) 195.
[16] G. Jacobs, E. Chenu, P.M. Patterson and L. Williams, Appl. Catal. A 258 (2004) 203.
[17] L. Kundakovic, D.R. Mullins and S.H. Overbury, Surf. Sci. 457 (2000) 51.